Zuse Institute Berlin

Takustrasse 7
D-14195 Berlin-Dahlem
Germany

MARTIN HAMMERSCHMIDT, CARLO BARTH, JAN POMPLUN, SVEN BURGER,
CHRISTIANE BECKER, FRANK SCHMIDT

Reconstruction of photonic crystal geometries using a reduced basis method for nonlinear outputs

This paper is made available as an electronic preprint with permission of SPIE and will be published in Proc. SPIE 9756 (2016). The full citation reads:
Martin Hammerschmidt, Carlo Barth, Jan Pomplun, Sven Burger, Christiane Becker and Frank Schmidt, "Reconstruction of photonic crystal geometries using a reduced basis method for nonlinear outputs", Proc. SPIE 9756, Photonic and Phononic Properties of Engineered Nanostructures VI, (2016).

ZIB Report 16-06 (January 2016)

Zuse Institute Berlin
Takustrasse 7
D-14195 Berlin-Dahlem

Telefon: 030-84185-0
Telefax: 030-84185-125

e-mail: bibliothek@zib.de
URL: http://www.zib.de

ZIB-Report (Print) ISSN 1438-0064
ZIB-Report (Internet) ISSN 2192-7782

Reconstruction of photonic crystal geometries using a reduced basis method for nonlinear outputs

Martin Hammerschmidt[a], Carlo Barth[a,b], Jan Pomplun[c], Sven Burger[a,c], Christiane Becker[b], Frank Schmidt[a,c]

[a]Zuse Institute Berlin, Takustraße 7, 14195 Berlin, Germany
[b]Helmholtzzentrum für Materialien und Energie, Kekuléstraße 5, 12489 Berlin, Germany
[c]JCMwave GmbH, Bolivarallee 22, 14050 Berlin, Germany

This paper is made available as an electronic preprint with permission of SPIE and will be published in Proc. SPIE 9756 (2016). The full citation reads:
Martin Hammerschmidt, Carlo Barth, Jan Pomplun, Sven Burger, Christiane Becker, Frank Schmidt, "Reconstruction of photonic crystal geometries using a reduced basis method for nonlinear outputs", Proc. SPIE 9756, Photonic and Phononic Properties of Engineered Nanostructures VI,(2016).

ABSTRACT

Maxwell solvers based on the hp-adaptive finite element method allow for accurate geometrical modeling and high numerical accuracy. These features are indispensable for the optimization of optical properties or reconstruction of parameters through inverse processes. High computational complexity prohibits the evaluation of the solution for many parameters. We present a reduced basis method (RBM) for the time-harmonic electromagnetic scattering problem allowing to compute solutions for a parameter configuration orders of magnitude faster. The RBM allows to evaluate linear and nonlinear outputs of interest like Fourier transform or the enhancement of the electromagnetic field in milliseconds. We apply the RBM to compute light-scattering off two dimensional photonic crystal structures made of silicon and reconstruct geometrical parameters.

Keywords: finite element method, rigorous optical modeling, photonic crystals, reduced basis method, reduced order models, parameter estimation, optical metrology

1. INTRODUCTION

Optical critical dimension metrology is used in the semiconductor industry to detect (sub-) nanometer sized features and deviations in quality and process control.[1] Measurements of scattered light from possibly complicated illumination setups are compared to the output of parameterized numerical models of the very same setup.[2] The method thus strongly relies on the availability of electromagnetic magnetic field solvers[3] to not only provide very accurate geometrical modeling and numerical solutions, but also to provide solutions in milliseconds for process control applications. Finite-element based solvers allow for high efficiency due the inherent flexibility and adaptivity in meshing and choice of the ansatz functions.[4] These methods usually outperform other rigorous electromagnetic field solvers.[5] However, high computational complexity prohibits the evaluation of the solution for many parameters in many cases.

We present a reduced basis method (RBM) for the time-harmonic electromagnetic scattering problem[6,7] allowing to compute solutions for a parameter configuration orders of magnitude faster than the underlying finite element solution. This model order reduction technique allows to evaluate linear and nonlinear outputs of interest such as Fourier transform or the enhancement of the electromagnetic field in milliseconds.[8–10] In this

Further author information: (Send correspondence to Martin Hammerschmidt)
Martin Hammerschmidt: E-mail: hammerschmidt@zib.de, Telephone: +49 30 84185-149

paper we apply the RBM to compute light-scattering off two dimensional photonic crystal structures made of silicon[11] and reconstruct geometrical parameters from reflectance measurements.

This paper is structured as follows: A brief summary of electromagnetic field simulations with a reduced basis is presented in Section 2. The optical model of the photonic crystal structure under investigation is presented in detail in Section 3. The results of the parameter reconstruction using the reduced basis are presented in Section 4.

2. ELECTROMAGNETIC FIELD SIMULATIONS WITH A REDUCED BASIS

In the following we briefly summarize the main ideas of the finite element method (FEM)[3,12,13] and the reduced basis method (RBM)[6,7,14,15] which is one of the most widely used model order reduction methods.[9,10,16,17] We refer to the references for an in depth presentation and discussion of the method. A detailed presentation of the method for the structure under investigation in this work has already been published.[9]

The linear Maxwell's equations describe scattering of monochromatic light by nano-structures. Assuming sinusoidal time-dependence, they are reformulated into a second order curl-curl equation for the electric field $\boldsymbol{E}$

$$\nabla \times \mu^{-1} \nabla \times \boldsymbol{E} - \omega^2 \varepsilon \boldsymbol{E} = 0 \tag{1}$$

over the computational domain Ω with the permeability and permittivity tensors μ and ε. ω is the frequency of the time-harmonic field and the exterior $\Omega_{ext} = \mathbb{R}^3 \setminus \Omega$ hosts incoming electric fields which act as sources in the interior Ω. We employ perfectly matched layers (PML) as a transparent boundary conditions at the boundary Γ of Ω.

The weak formulation of (1) is the starting point for the FEM discretization. It reads:
Find $\boldsymbol{E} \in V_h$ such that:

$$a(\varphi, \boldsymbol{E}) = f(\varphi) \quad \forall \varphi \in V_h. \tag{2}$$

The finite element space V_h is spanned by polynomial ansatz functions over geometrical patches belonging to a discretization of the computational domain Ω. The solution $\boldsymbol{E}$ is a linear combination of the ansatz functions spanning V_h. The local support of the basis function leads to a sparse linear system with $\mathcal{N}$ degrees of freedom to be solved for the coefficients of $\boldsymbol{E}$ in V_h.

Although FEM allows for meshes and polynomial degrees to be adapted to suit the properties of the structures under investigation,[4,13] oftentimes the computational effort demanded by the simulations render extensive studies or optimizations infeasible and rule out real-time applications such as on-line process control. In these situations reduced order models, provided for example by the reduced basis method, are of great importance. They offer a way to construct error controlled approximations to map inputs, such as specific configuration of parameters $\mu \in \mathbb{R}^d$, to output quantities $s(\mu) = s(\boldsymbol{E}(\mu))$ derived from a solution $\boldsymbol{E}$ of the parameter dependent partial differential equation (1).

The RBM works in two phases: First, a reduced basis space X is built self-adaptively from so-called snapshot solutions. These are computed by solving the full FEM problem for specific parameter configurations. Subsequently, the finite element space V_h in (2) is replaced by this reduced space X. The resulting linear system is independent of $\mathcal{N}$ and only depends on the dimension $N << \mathcal{N}$ of the reduced space. This system can be solved in milliseconds. The reduced basis solution is a very low dimensional approximation to solutions of the high dimensional problem (2). The approximation errors are usually only controlled for parameters μ within a bounded domain $\mathfrak{D} \subset \mathbb{R}^d$. As noted above, the construction phase of the reduced basis requires multiple solutions of the full problem to be computed and this carries significant computational effort, but this step has to be executed only once. This step is called the *offline* phase. The second or *online* phase only requires the reduced model and the solution are obtained orders of magnitude faster.

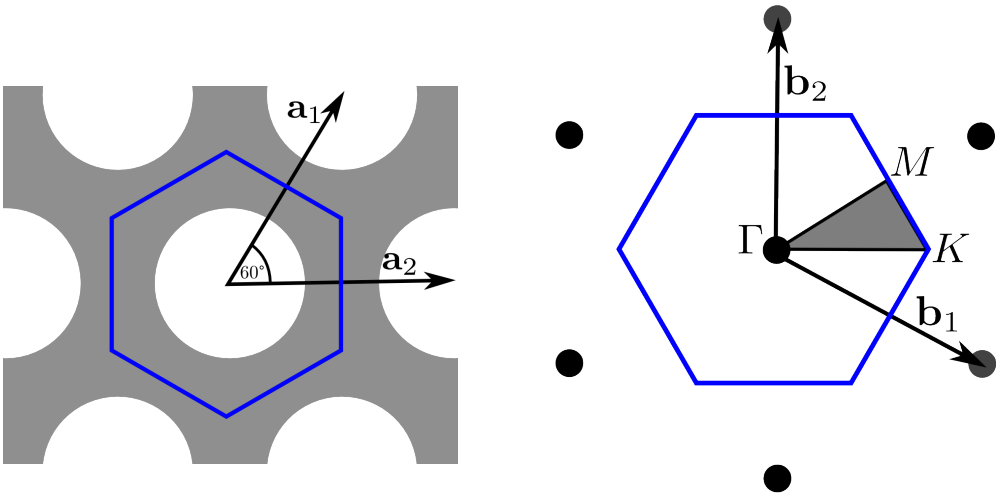

(a) (b)

Figure 1: Schematic of the unit cell of the hexagonal nanohole array with 600 nm pitch in real space (a) and k-space (b). The high-symmetry points of the irreducible Brillouin zone (gray) are marked.

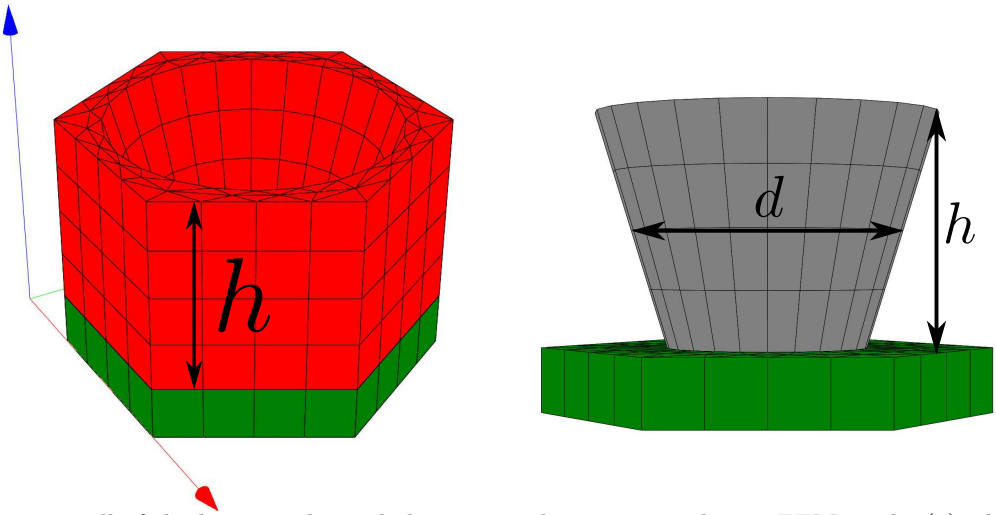

(a) (b)

Figure 2: The unit cell of the hexagonal nanohole array with 600 nm pitch as a FEM mesh. (a) The silicon slab (red) sits on a glass substrate (green) and is h=360 nm thick. An air layer above (100 nm thick, not shown) completes the cell. In $\pm z$ directions transparent boundary conditions are applied. (b) A side view of the conical hole (gray) centered in the unit cell with a sidewall angle of 17°. It has a diameter d of of 405 nm at the center of the slab.

3. OPTICAL MODEL FOR A 2D PHOTONIC CRYSTAL MADE OF SILICON

In this section we present an optical model of a 2D photonic crystal made of silicon. Photonic crystals exhibit a photonic band gap, a specific frequency interval in which propagation of light or more general electromagnetic waves are inhibited. This is usually achieved through repeating material patterns or nano-structuring such as the introduction of gratings. A frequently investigated pattern is that of conical (air) holes in a high-index substrate such as silicon arranged in a hexagonal array. They are envisioned to be employed in various applications ranging from light management or up-conversion in solar cells to enhancement of optical sensing.

The optical model presented here is a parameterized version of a model used in previous publications.[9,11] In Figure 1 the outline of the unit cell of the 2D crystal is shown in real (a) and k-space (b) with the boundary of the cell and irreducible Brillouin zone marked. High-symmetry points are also marked. In Figure 2 (a) a FEM mesh of the unit cell is depicted in oblique view. The silicon slab (red) sits on a glass substrate (green) and is h=360 nm thick. An air layer fills the hole and is extended 100 nm above the substrate. For the purpose of visualization this domain is not shown. The height h of the slab is indicated. In Figure 2 (b) a side view of the unit cell is shown. In this representation the hole domain is shown and the definition of the hole diameter d measured at the center of the slab is indicated as well as the height h of the slab. The silicon slab is omitted in this view.

The unit cell is modeled as an infinitely extended periodic array of holes, i.e. periodic boundary conditions are applied. In $\pm z$ directions transparent boundary conditions are realized with perfectly matched layers.[18] The illumination is given by a p-polarized plane wave with wavelength λ incident from the upper half space. The incidence angle ϑ is measured with respect to the $\Gamma - K$ direction. The optical data for the simulations is taken from the literature[19] but optical losses in the infrared part of the spectrum are neglected, i.e. the refractive index is assumed to be real-valued. $n_{air} = 1$ and $n_{glass} = 1.53$ are kept constant. The FEM discretization uses second order elements.

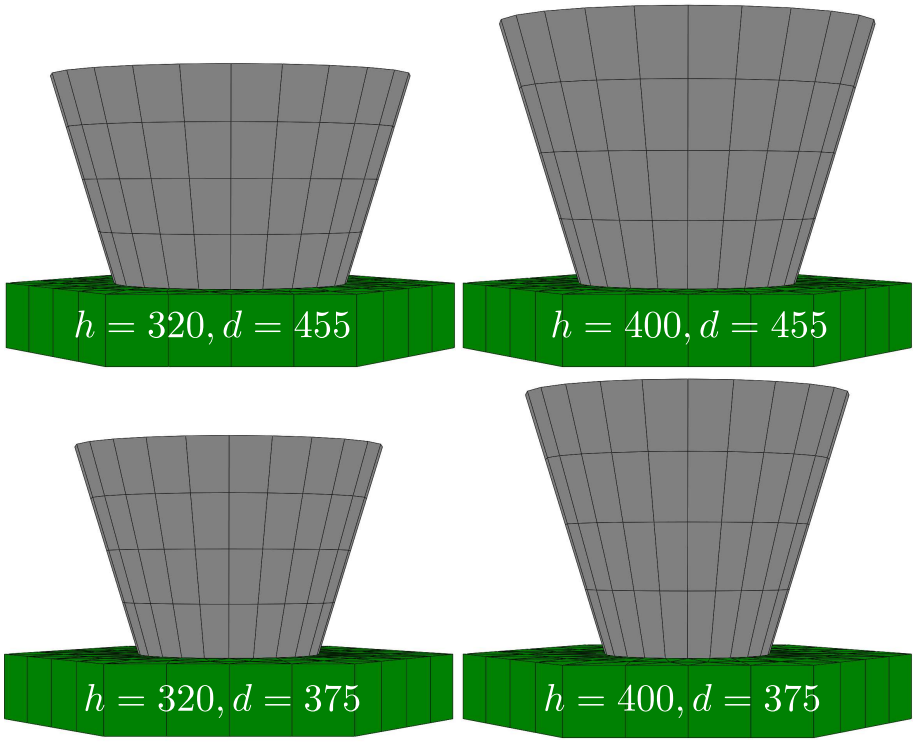

Figure 3: Projections of the FEM mesh of the parameterized unit cell of the hexagonal nanohole for the corners of the parameter space $\mathfrak{D}$. To facilitate comparison only the conical hole is shown, i.e. the slab is omitted. The parameters are in (a) h=320 nm, d=455 nm, (b) h=400 nm, d=455 nm, (c) h=320 nm, d=375 nm and (d) h=400 nm, d=375 nm.

In order for the reduced basis method to vary geometrical parameters such as the slab height h and the nanohole diameter d, the FEM mesh must be parameterized. The parameterization of the mesh must yield topologically equivalent FEM meshes for every parameter $\mu \in \mathfrak{D}$ considered. In the example considered here, this can readily be achieved by the meshing tools integrated in our FEM toolbox JCMsuite.[20] However, generating these parameterizations can become very involved when more complex nanostructures, such as fin field-effect transistors are investigated.[10,21]

In Figure 3 projections of the parameterized mesh are shown. The mesh is set to the corners of the parameter space $\mathfrak{D}$ used in the Section 4. The parameter values for h and d are indicated in the plots. The sidewall angle is not changed. The projections in this Figure demonstrate the different aspect ratios the structure can adopt. Furthermore, it demonstrates the flexibility of the mesh as all of the shown projections are topologically equivalent which is of significant importance for the reduced basis method.

4. GEOMETRY RECONSTRUCTION USING A REDUCED BASIS

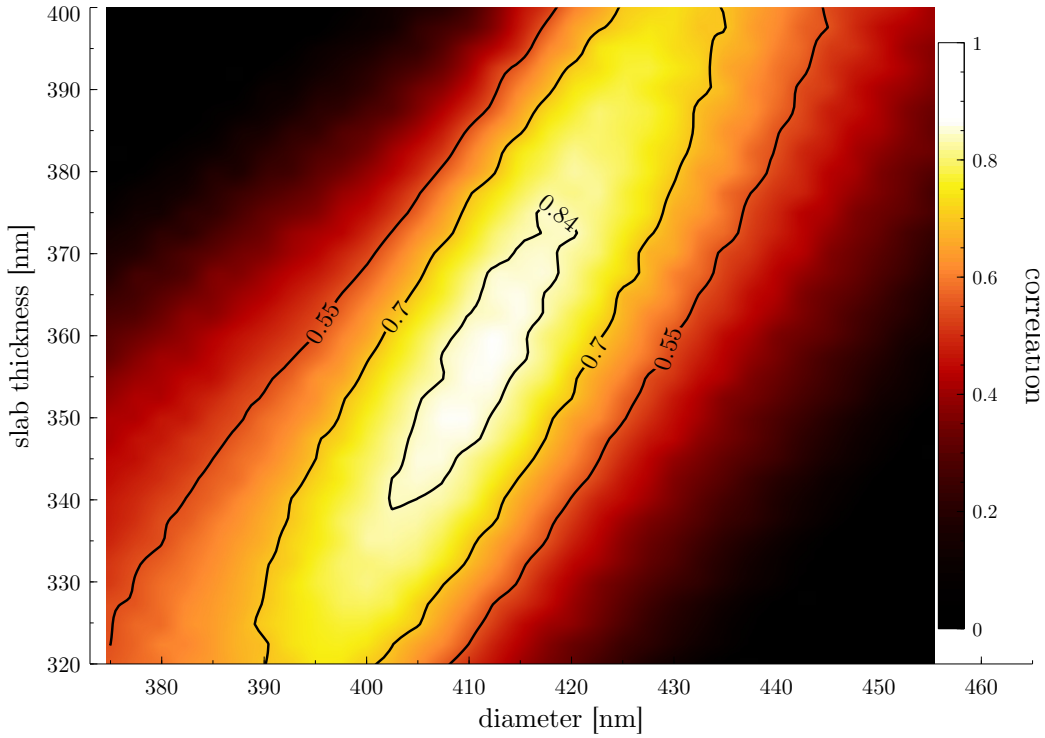

Figure 4: Correlation ρ of simulated and measured reflectance over the parameter space $\mathfrak{D}$. Contour lines for $\rho = 0.55$,$\rho = 0.7$ and $\rho = 0.84$ are also shown. The maximum of $\rho = .87$ is found for $d = 412.5$ nm and $h = 360$ nm within an ellipsoidal region of high correlation.

In a previous study[11] we observed a red shift of 50-100 nm of the resonance positions between simulations and experimental measurements. In the cited reference we attributed the deviations to differences in the geometry parameters employed for the simulations. In the following we thus try to reconstruct or estimate the correct model parameters, the diameter of the conical hole d at the center of the slab and the thickness h of the slab, to fit the experimental data. We use the cross correlation between measured and simulated reflectance spectra as the figure of merit.

We select four incidence angles $\vartheta \in \{20, 36, 50, 60\}$ and a wavelength interval $\Lambda = [1000\text{ nm}, 1600\text{ nm}]$ for the figure of merit. The selection of Λ is informed by the presence of several distinct resonances in both the measurements and simulations. The selection of the incidence angles allows to observe the shift of the resonances with the illumination angle. We employ reduced bases for the geometrical parameters h and d to make a high density sampling of these parameters feasible within the parameter space $\mathfrak{D} = [320\text{ nm}, 400\text{ nm}] \times$

[375 nm, 455 nm]. Hence, we constructed 404 reduced bases for each of the incidence angles ϑ and a wavelength sampling of 6 nm in Λ. We note, that strategies exist to build a single reduced model[22] instead of multiple bases, but this implementation is much more involved. We limit the bases to at most 30 snapshots each to limit online evaluation time and to limit construction times. On average we require 22.8 snapshot to reach an estimated error of less than 1 % in all of the bases. The maximum estimated error over $\mathfrak{D}$ is $1.64 \cdot 10^{-4}$ on average. The error estimate was found to be highly correlated to the actual simulation error in previous studies.[9,10,15] Hence we are confident, that our simulations results are accurate to at least a level of $1 \cdot 10^{-3}$ in the output quantities.

The reduced basis method allows to evaluate the parameter dependent solution of the reduced problem in milliseconds of CPU time. This drastically reduces the computational effort for a dense sampling of the parameter space $\mathfrak{D}$. We note, that a sampling or grid based optimization algorithm is not an optimal choice in terms of efficiency. Newton-type methods allow to find the optimal solutions with fewer evaluations of the function of merit. Evolutionary optimization algorithm are guaranteed to find global minima, like the grid based approach used here, but may not have optimal complexity. Either type of optimization algorithm can benefit from the speedup gained by a reduced model. We chose the grid based strategy for its simplicity and advantages in visualizing the parameter trends.

To compute the cross correlation ρ between the measured and simulated reflectance spectra for the investigated incidence angles we thus evaluate the reduced models for a parameter configuration and combine the results. Subsequently we employ a centered moving average (MA) filter over three data points of the computed spectra and compute the cross correlation between the measured and the simulated and filtered spectra in Matlab. Figure 4 depicts the obtained correlation ρ over the parameter space $\mathfrak{D}$. The parameter location of the maximum ($\rho = .87$) for $d = 412.5$ nm and $h = 360$ nm is not isolated and readily recognizable. Instead, we find an ellipsoidal region of correlation $\rho > 0.84$ centered around this location. Any parameter configuration within this region gives approximately the same correlation to the measured spectra. Hence we have a high sensitivity of the maximum with respect to errors in the measurement and simulations. We note that the choice of averaging the simulated spectra leads to an overall increased correlation, but not to a different shape of the contour lines shown in Figure 4. As the measurements itself is not executed with perfectly monochromatic light and we observe slight imperfections in the experimentally realized photonic crystal, the measurement can be seen as an incoherent average of different spectra. This effect is reflected by the use of the moving average filter. The effect of this filter is observable in Figure 5. Here, the simulated and measured spectra for the four different incidence angles ϑ are shown together. The measured spectra (black solid lines) and simulated and filtered spectra (red solid lines) of the optimal parameters d and h are highly correlated and the wavelength positions of the reflectance maxima are almost perfectly aligned. The filter smooths the actual simulation data (shown as dashed red lines), i.e. it limits the amplitudes of the simulated peaks while broadening the resonances. This better reflects the measurement as mentioned above. Still, all resonances observed in the measurements are still present although some smaller peaks can merge into a single, broader resonance (cf. $\vartheta = 36°$at 1200 nm).

In Figure 6 the measured and simulated reflectance spectra are shown over of the incidence angle and wavelength for both polarizations. Here, the simulated reflectance is obtained from over 30 000 FEM scattering simulations for the best-fit parameters found in the reconstruction process. The simulated reflectance is shown in this Figure with an inverted angle axis to facilitate the observation of the symmetry in both spectra. The p-polarization is shown in the upper plots and the s-polarization in the lower. We observe almost exact alignment of the visible resonance bands over the complete spectrum. The alignment is best observed at 70° where the plots touch.

4.1 Field enhancement computation using nonlinear outputs of interest from a RBM

As in previous studies[9,11] we compute near-field enhancements in the conical nanohole as an increased electromagnetic field energy density in the hole domain and a 100 nm thick layer above the silicon slab. We normalize the enhancements by the same quantity for an undisturbed incident field in free space. The resonance bands observed in the experimental results could be correlated to resonance modes of the photonic crystal[11] and high field enhancements were observed.

The reduced basis method not only allows for linear outputs such as the Fourier transform of the electromagnetic field to be computed (from which the reflectance is inferred), but our implementation also allows for

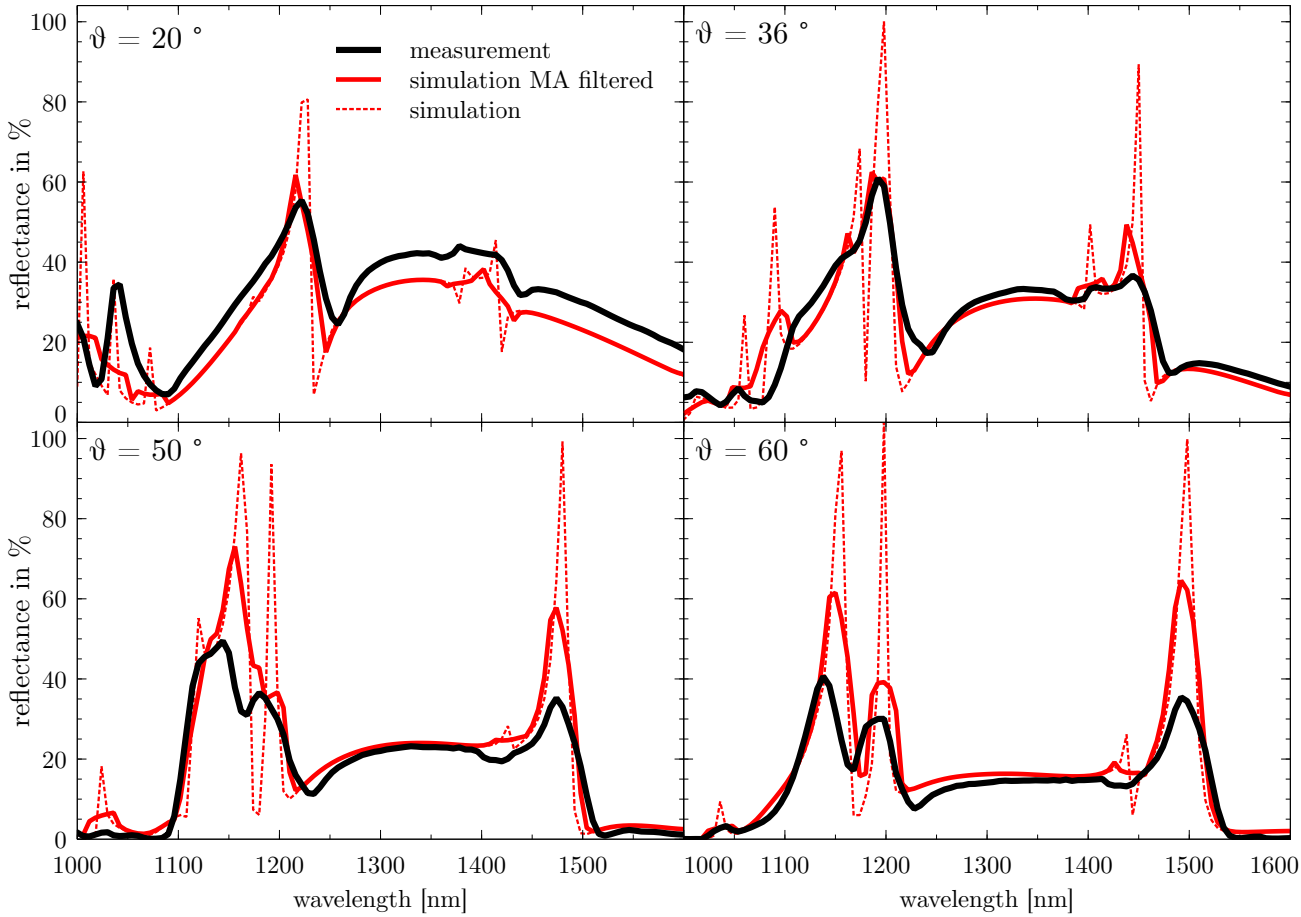

Figure 5: Reflectance spectra of the nanohole array for four incidence angles ϑ as noted in the upper left corner of each axis. The measured reflectance is shown as a solid black line. The simulation for the reconstructed parameters is depicted as a dotted red line. The MA filtered simulation data (red solid line) replicates the features of measurements well, whereas the extrema observed in the simulations are less pronounced in the measurements.

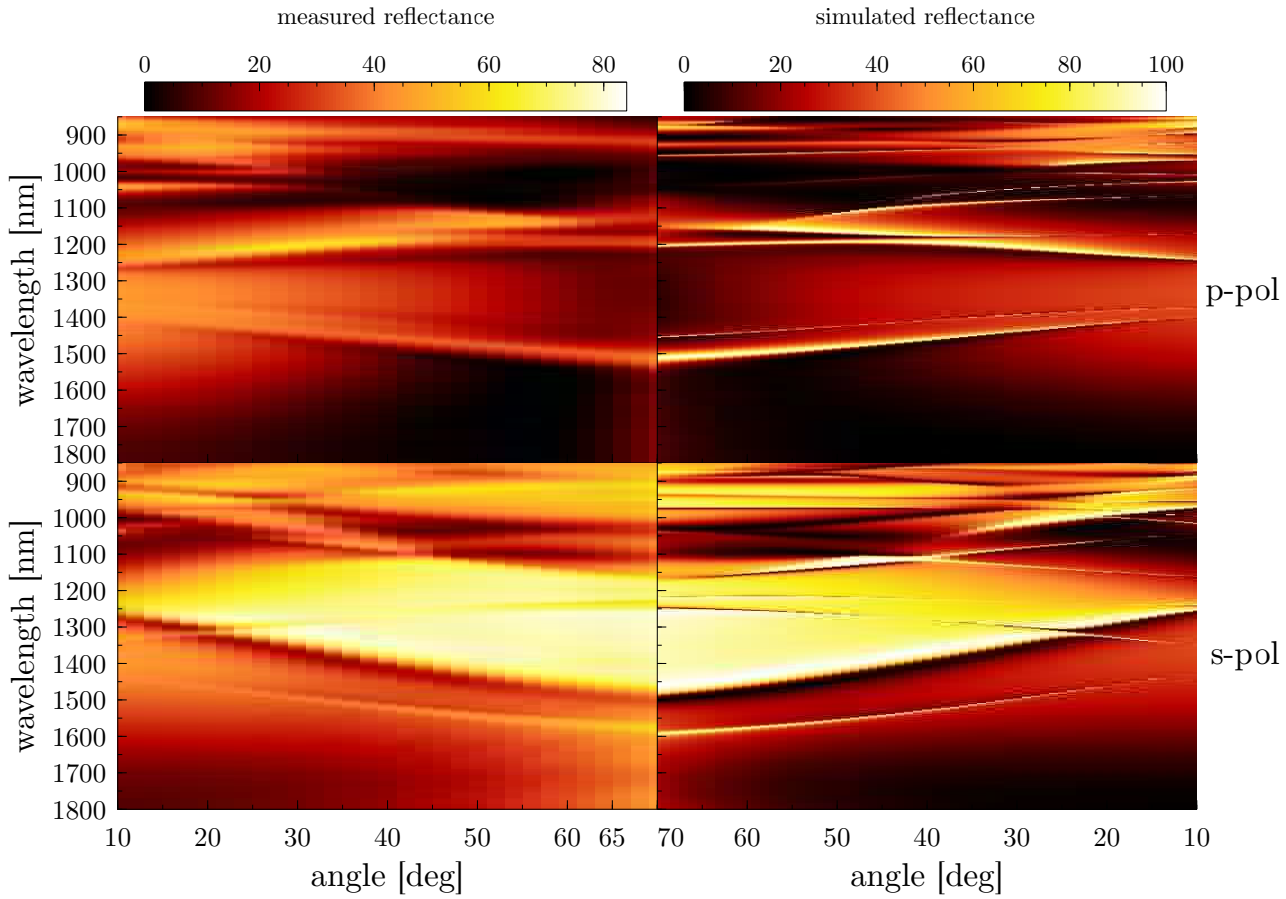

Figure 6: Comparison of simulated and reflected reflectance spectra of the nanohole array over incidence angle and wavelength for both polarizations. The simulated reflectance is shown with an inverted angle axis to facilitate the observation of the symmetry in both spectra. The p-polarization is shown in the upper plots and the s-polarization in the lower. We observe almost exact alignment of the visible resonance bands over the complete spectrum. The alignment is best observed at 70° where the plots touch.

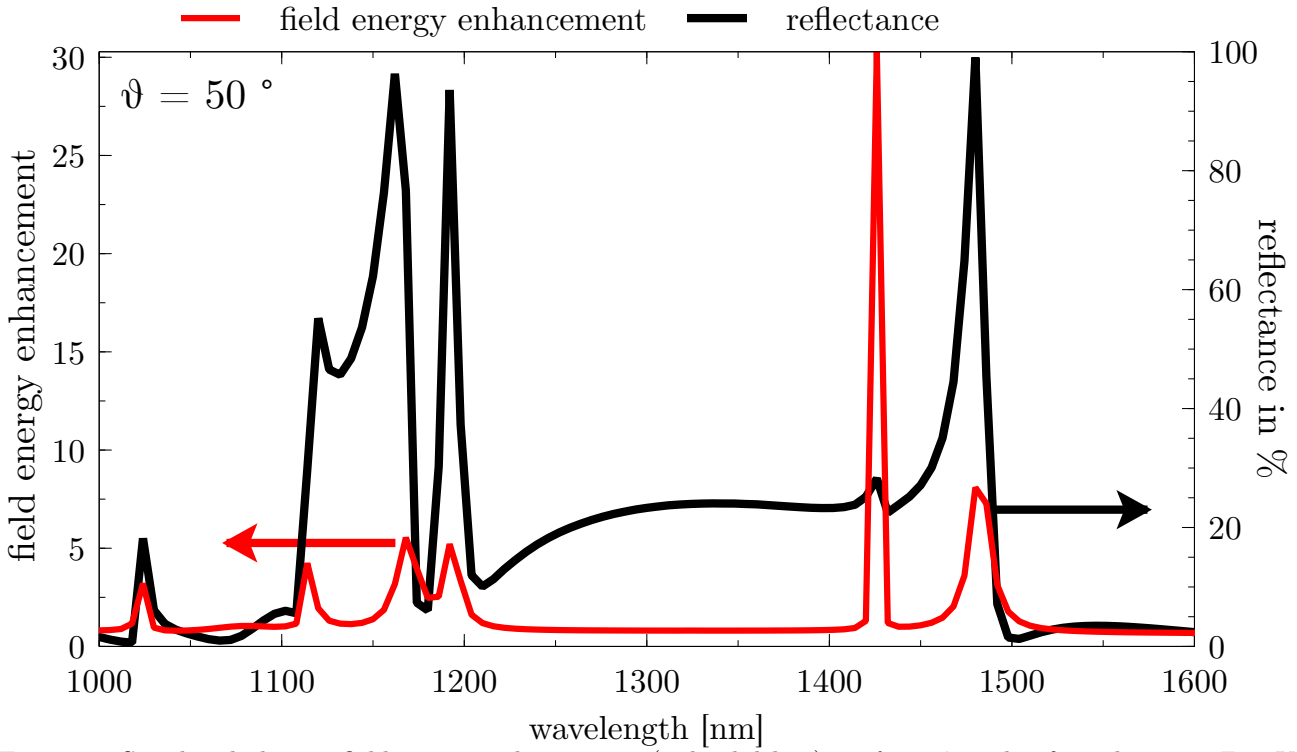

Figure 7: Simulated electric field energy enhancement (red solid line) at ϑ =50° angle of incidence in $\Gamma - K$ direction for p-polarized light for $d = 412.5$ nm and $h = 360$ nm. The simulated reflectance is shown as a solid black line. The arrows indicated the respective axis. The resonance positions of the simulated field enhancement and reflectance coincide.

the evaluation of nonlinear outputs. The additional costs for the online evaluation are higher ($O(N^2)$ instead of $O(N)$ for a linear quantity), but nevertheless the evaluation in the online phase is done in milliseconds. Theoretically, this allows for an inverse problem to be solved based on a nonlinear instead of a linear quantity in the same time. However, it requires also a measurement of the same quantity to compare to.

The structure under investigation exhibits several distinct resonances in the field energy enhancement as defined above. Like in the reflectance, the resonances in the field energy enhancement shift in wavelength and vary in shape with changing d and h. In Figure 7 the simulated field energy enhancement for the parameters $d = 412.5$ nm and $h = 360$ nm is shown over the wavelength. The simulated reflectance without the moving average filtering is shown in the same graph on a different axis. We observe a good agreement in the resonance positions of the simulated field energy enhancement and reflectance. We note, that the maximum field enhancement of 30.28 at 1426 nm is found at a seemingly small resonance of the reflectance. This might indicate a very narrow band resonance which is not properly resolved by the chosen sampling of the wavelength.

The computed field enhancements give additional insight into the electromagnetic near field. The sharp peaks correspond to Bloch modes in the photonic crystal. The field energy enhancement gives an indication of the leakage into the conical hole. Depending on the application in mind, e.g. optical sensing or upconversion, the reduced basis presented here could also be used to optimize photonic crystal geometry to achieve high field energy enhancements for specific modes. This would be advantageous for the applications above where high field intensities are required.

5. CONCLUSION

Reconstructed parameters for a photonic crystal geometry have been found through an inverse process of optical critical dimension metrology. We no longer observe a significant shift in the resonance positions as present in a

previous study[11] without the parameter reconstruction. The reduced basis method has proven to be a reliable and efficient tool in obtaining the forward solution of the parameterized electromagnetic scattering problem. The availability of nonlinear output quantities allows to gain additional insight into the physical properties of the structure.

ACKNOWLEDGMENTS

The results were obtained at the Berlin Joint Lab for Optical Simulations for Energy Research (BerOSE) of Helmholtz-Zentrum Berlin für Materialien und Energie, Zuse Institute Berlin and Freie Universität Berlin. This research was carried out in the framework of MATHEON supported by Einstein Foundation Berlin through ECMath within subproject SE6.

REFERENCES

[1] Bunday, B., Germer, T. a., Vartanian, V., Cordes, A., Cepler, A., and Settens, C., "Gaps analysis for CD metrology beyond the 22nm node," *Proc. SPIE* **8681** (2013).

[2] Pang, L., Peng, D., Hu, P., Chen, D., He, L., Li, Y., Satake, M., and Tolani, V., "Computational metrology and inspection (CMI) in mask inspection, metrology, review, and repair," *Advanced Optical Technologies* **1**(4) (2012).

[3] Lavrinenko, A. V., Laegsgaard, J., Gregersen, N., Schmidt, F., and Soendergaard, T., [*Numerical Methods in Photonics*], CRC Press (2014).

[4] Burger, S., Zschiedrich, L., Pomplun, J., Herrmann, S., and Schmidt, F., "Hp-finite element method for simulating light scattering from complex 3D structures," *Proc. SPIE* **9424** (2015).

[5] Maes, B., Petráček, J., Burger, S., Kwiecien, P., Luksch, J., and Richter, I., "Simulations of high-Q optical nanocavities with a gradual 1D bandgap," *Optics Express* **21**(6) (2013).

[6] Rozza, G., Huynh, D. B. P., and Patera, A. T., "Reduced Basis Approximation and a Posteriori Error Estimation for Affinely Parametrized Elliptic Coercive Partial Differential Equations," *Archives of Computational Methods in Engineering* **15**(3) (2008).

[7] Pomplun, J. and Schmidt, F., "Accelerated a posteriori error estimation for the reduced basis method with application to 3D electromagnetic scattering problems," *SIAM J. Sci. Comput.* **32** (2010).

[8] Kleemann, B. H., Kurz, J., Hetzler, J., Pomplun, J., Burger, S., Zschiedrich, L., and Schmidt, F., "Fast online inverse scattering with reduced basis method (RBM) for a 3D phase grating with specific line roughness," *Proc. SPIE* **8083** (2011).

[9] Hammerschmidt, M., Herrmann, S., Pomplun, J., Zschiedrich, L., Burger, S., and Schmidt, F., "Reduced basis method for Maxwell's equations with resonance phenomena," *Proc. SPIE* **9630** (2015).

[10] Hammerschmidt, M., Herrmann, S., Burger, S., Pomplun, J., and Schmidt, F., "Reduced basis method for the electromagnetic scattering problem: a case study for FinFETs (accepted)," *Optical and Quantum Electronics* **48**(2) (2016).

[11] Becker, C., Wyss, P., Eisenhauer, D., Probst, J., Preidel, V., Hammerschmidt, M., and Burger, S., "5 x 5 cm^2 silicon photonic crystal slabs on glass and plastic foil exhibiting broadband absorption and high-intensity near-fields," *Scientific reports* **4** (2014).

[12] Monk, P., [*Finite Element Methods for Maxwell's Equations*], Numerical Mathematics and Scientific Computation, Clarendon Press (2003).

[13] Demkowicz, L. F., Kurtz, J., Pardo, D., Paszenski, M., Rachowicz, W., and Zdunek, A., [*Computing with hp-ADAPTIVE FINITE ELEMENTS: Volume II Frontiers: Three Dimensional Elliptic and Maxwell Problems with Applications*], Chapman & Hall/CRC Applied Mathematics & Nonlinear Science, CRC Press (2007).

[14] Prudhomme, C., Rovas, D. V., Veroy, K., Machiels, L., Maday, Y., Patera, A. T., and Turinici, G., "Reliable Real-Time Solution of Parametrized Partial Differential Equations: Reduced-Basis Output Bound Methods," *Journal of Fluids Engineering* **124**(1) (2002).

[15] Pomplun, J., *Reduced basis method for electromagnetic scattering problems*, phd thesis, Freie Universität Berlin (2010).

[16] Schmidt, F., Pomplun, J., Zschiedrich, L., and Burger, S., "Fast online simulation of 3D nanophotonic structures by the reduced basis method," *Proc. SPIE* **7941** (2011).

[17] Pomplun, J., Burger, S., Zschiedrich, L., and Schmidt, F., "Reduced basis method for real-time inverse scatterometry," *Proc. SPIE* **8083** (2011).

[18] Zschiedrich, L., *Transparent boundary conditions for Maxwells equations: numerical concepts beyond the PML method*, phd thesis, Freie Universität Berlin (2009).

[19] Palik, E. D., [*Handbook of Optical Constants of Solids*], Academic Press handbook series, Academic Press (1998).

[20] Pomplun, J., Burger, S., Zschiedrich, L., and Schmidt, F., "Adaptive Finite Element Method for Simulation of Optical Nano Structures," *Physica Status Solidi (B)* **244**(10) (2007).

[21] Hammerschmidt, M., Herrmann, S., Pomplun, J., Burger, S., and Schmidt, F., "Model order reduction for the time-harmonic Maxwell equation applied to complex nanostructures," *Proc. SPIE* **9742** (2016).

[22] Eftang, J. L., Patera, A. T., and Rønquist, E. M., "An "hp" Certified Reduced Basis Method for Parametrized Elliptic Partial Differential Equations," *SIAM Journal on Scientific Computing* **32**(6) (2010).